HHS Public Access

Author manuscript

Nat Struct Mol Biol. Author manuscript; available in PMC 2012 January 01.

Published in final edited form as:

Nat Struct Mol Biol. ; 18(7): 761–768. doi:10.1038/nsmb.2078.

Chfr and RNF8 synergistically regulate ATM activation

Jiaxue Wu[1], **Yibin Chen**[1], **Lin-Yu Lu**[1], **Yipin Wu**[2], **Michelle T. Paulsen**[3], **Mats Ljungman**[3], **David O Ferguson**[2], and **Xiaochun Yu**[1]

[1] Division of Molecular Medicine and Genetics, Department of Internal Medicine, University of Michigan Medical School, Ann Arbor, Michigan 48109, USA

[2] Department of Pathology, University of Michigan Medical School, Ann Arbor, Michigan 48109, USA

[3] Department of Radiation Oncology, University of Michigan Medical School, Ann Arbor, Michigan 48109, USA

Abstract

Protein ubiquitination is a critical component of the DNA damage response. To study the mechanism of the DNA damage-induced ubiquitination pathway, we analyzed the impact of the loss of two E3 ubiquitin ligases, RNF8 and Chfr. Interestingly, DNA damage-induced ATM activation is suppressed in RNF8 and Chfr double-deficient (DKO) cells, and DKO mice develop thymic lymphomas that are nearly diploid but harbor clonal chromosome translocations. Moreover, DKO mice and cells are hypersensitive to ionizing radiation. We show evidence that RNF8 and Chfr synergistically regulate histone ubiquitination to control histone H4K16 acetylation through MRG15-dependent acetyltransferase complexes. Through these complexes, RNF8 and CHFR affect chromatin relaxation and modulate ATM activation and DNA damage response pathways. Collectively, our findings demonstrate that two chromatin remodeling factors, RNF8 and Chfr, function together to activate ATM and maintain genomic stability *in vivo*.

Introduction

Cells encounter numerous exogenous and endogenous factors, under both pathological and physiological conditions, that cause DNA lesions such as double-strand breaks (DSBs). In response to DSBs, highly conserved signal transduction pathways are activated to delay cell cycle progression and repair DNA lesions [1, 2]. Abrogation of the DNA damage response (DDR) caused by genetic mutations in key DDR players often leads to genomic instability and ultimately induces tumor development [3]. One example is Ataxia Telangiectasia Mutated (ATM), a key PI3 kinase that dictates protein phosphorylation events in response to DSBs generated under genotoxic stress as well during normal development [4–7]. When DSBs occur,

Correspondence should be addressed to: X.Y. (xiayu@umich.edu).

Author Contributions

J.W. performed most experiments. Y.C. analyzed the MRG15-related protein-protein interactions. L.L., M.P.T., M.L., Y.W. and D.O.F provided technical support on various assays. X.Y. designed the experiments. X.Y. and J.W. wrote the manuscript. All the authors read and approved the final manuscript.

ATM is quickly activated and arrests the cell cycle through its associated signal transduction pathways, which facilitate DNA damage repair [4–7]. Cells derived from Ataxia-telangiectasia patients and ATM-deficient mice are hypersensitive to genotoxic agents such as ionizing radiation (IR) [8, 9]. Correspondingly, ATM-mutation carriers are predisposed to lymphatic leukemia [10], and ATM-deficient mice are prone to T-cell lymphoma [8, 9, 11].

DNA damage response is not only controlled by ATM and other PI3 kinase-associated protein phosphorylation cascades, but also regulated by recently identified protein ubiquitination events [12, 13]. One of the key E3 ubiquitin ligases that governs DNA damage-induced protein ubiquitination is RNF8 (Ring finger protein 8) [14–17]. RNF8 is a 485-residue nuclear polypeptide with an N-terminal FHA domain and a C-terminal Ring domain [18]. In response to DSBs, the FHA domain of RNF8 recognizes three phospho-Thr motifs on MDC1, a partner of γH2AX, thus targeting RNF8 to DNA lesions [14–16]. The Ring domain of RNF8 functions together with Ubc13, an E2 ubiquitin conjugase, to initiate histone ubiquitination at DNA damage sites [19], and recruits other downstream E3 ligases such as RNF168, Herc2 and Rad18 to amplify the protein ubiquitination signals [12]. These ubiquitination events are critical for the localization of other DDR factors including RAP80/BRCA1 complex and 53BP1 in response to DSBs, and facilitate DNA damage checkpoint activation and DNA damage repair [12, 13].

Interestingly, RNF8 shares similar domain architecture with Chfr (checkpoint protein with FHA and Ring domain), a nuclear E3 ubiquitin ligase with potentially multiple functions [20]. Like RNF8, the E2 partner of Chfr is also Ubc13 [21], the key enzymatic subunit needed to catalyze histone ubiquitination at DNA damage sites [19]. Moreover, Chfr is downregulated in 20 ~ 40% of primary tumors and tumor cell lines, suggesting that Chfr may play a role in tumor suppression [22, 23].

Since RNF8 and Chfr share similar functional domains and interact with the same E2 ubiquitin conjugase, we wondered whether RNF8 and Chfr could be functional paralogs in the same biological processes. By analyzing RNF8 and Chfr-deficient mice, we find that RNF8 and Chfr synergistically maintain genomic stability and suppress tumor development *in vivo* by regulating histone modifications and the ATM-dependent DNA damage response pathway following DSBs. Our results demonstrate the *in vivo* functional significance and molecular mechanisms of a pair of FHA and Ring domain proteins.

Results

Loss of RNF8 and Chfr abrogates ATM-dependent DNA damage response

Both RNF8 and Chfr contain an N-terminal FHA domain and a Ring domain (Figure 1a). The Ring domains of RNF8 and Chfr are also functionally interchangeable [24]. Thus, the similar domain architecture of RNF8 and Chfr suggests that these two proteins may function in the same or similar biological processes. To examine potential functional correlations between RNF8 and Chfr, we crossed *RNF8* +/− mice with *Chfr* +/− mice, bred offspring to generate RNF8 and Chfr double-deficient (DKO) mice, and extracted mouse embryo fibroblasts (MEFs). To examine whether Chfr, like RNF8, plays a role in response to DNA damage, we examined the ATM-dependent phosphorylation of downstream targets p53,

Chk1/2, NBS1 and BRCA1 after induction of DSBs. Surprisingly, all of these ATM-dependent phosphorylation events were suppressed in DKO MEFs (Figure 1b), suggesting that Chfr and RNF8 might cooperate to facilitate ATM-dependent signal transduction following DNA damage. Next, we wondered whether DNA damage-induced ATM activation is impaired in DKO cells. As shown in Figure 1b and Supplementary Figure 1a, compared with that in wild type MEFs, autophosphorylation of ATM Ser1987, a surrogate marker of activated ATM [25], was dramatically reduced in DKO MEFs following DNA damage. Additionally, IR-induced ATM activation was dramatically suppressed in RNF8-depleted HCT116 and HCT15 cells (Supplementary Figure 1b), which do not express Chfr [26], Since ATM is important for T-cell development [8, 9], we also examined the DNA damage-induced ATM activation in primary thymocytes harvested from DKO mice. Again, IR-induced ATM activation was impaired (Figure 1c). Moreover, we performed *in vitro* ATM kinase assay and found the kinase activity of ATM was reduced in IR-treated DKO cells (Figure 1d), suggesting that RNF8 and Chfr regulate DNA damage-induced ATM activation. Next, we examined IR-induced G1/S and G2/M checkpoint activation controlled by ATM and its associated pathways [4–6]. As shown in Figure 1e and Supplementary Figure 1c, the G1/S checkpoint is disrupted in DKO MEFs. Similarly, the G2/M checkpoint is also abolished in DKO MEFs (Figure 1f and Supplementary Figure 1d). Collectively, these results suggest that RNF8 and Chfr are important for ATM activation and its downstream DNA damage response.

RNF8 and Chfr double-deficient mice develop T-cell lymphoma

To examine whether RNF8 and Chfr regulate ATM function *in vivo*, we generated a cohort containing 20 *RNF8* +/+ *Chfr* +/+ (wild type), 20 *RNF8* −/− *Chfr* +/+ (RNF8 KO), 20 *RNF8* +/+ *Chfr* −/− (Chfr KO) and 20 *RNF8* −/− *Chfr* −/− (DKO) mice. Interestingly, although DKO mice were viable, 40 % of DKO mice developed thymic lymphoma and became moribund within six months, whereas no tumor incidence or lethality was observed in the wild type, RNF8 KO or Chfr KO mice during this time (Figure 2a and b). Besides thymic lymphoma, we did not find any other type of tumor in DKO mice. Flow cytometry analysis showed that tumor cells from DKO mice were CD4 + CD8 + T cells, indicating that these lymphomas developed during the CD4CD8 double positive selection stage (Figure 2c). Histological examination showed that the tumor cells were large-size lymphoblasts. Mitotic figures were observed in tumor tissues, indicating the fast growth of these lymphomas (Figure 2d). Thus, these results suggest that the loss of RNF8 and Chfr induces lymphomagenesis *in vivo*, which is very similar to the phenotype of ATM −/− mice [8, 9].

Mouse chromosomes 12 and 14 are frequently altered in DKO lymphoma

Thymic lymphoma can be induced by multiple mechanisms including chromosome aneuploidy and clonal translocations. To elucidate the mechanism of T-cell lymphomagenesis in DKO mice, we examined the karyotype of five tumors from DKO thymuses. As listed in Figure 3, all five T-cell lymphomas display chromosomal translocations. Specifically, all five tumors contain abnormal rearrangements on chromosome 12 and/or 14. All of the analyzed tumors from DKO mice were diploid or close to diploid (Figure 3). Since we only found one karyotype per tumor sample, these lymphomas were likely induced by clonal translocation of chromosomes. Interestingly, these

tumor karyotypes are very similar to those in T-cell lymphomas of *ATM* −/− mice. Like DKO mice, *ATM* −/− mice develop CD4+ CD8+ T-cell lymphomas with clonal translocation involving chromosome 12 and 14 [8, 9, 11]. Moreover, mouse chromosome 12 and 14 are homologous to human chromosome 14, which is the site of frequent chromosome rearrangements in patients bearing ATM mutations [27–29]. These data indicate that the *in vivo* phenotype of DKO mimics that seen with ATM loss or mutation.

T cell development is impaired in DKO mice

Since T-cell lymphomas in *ATM* −/− mice are caused by abnormal T-cell development, we further examined thymic T-cells of DKO mice. Although no obvious tissue architecture defect was observed, the thymuses in DKO mice were much smaller than those in wild type mice, Chfr KO or RNF8 KO mice (data not shown). The thymus cellularity in DKO mice was reduced on average to 35% of that of wild type mice. No obvious loss of thymocyte was observed in Chfr KO mice, while a slight reduction of thymus cellularity was detected in RNF8 KO mice (Supplementary Figure 2a). Flow cytometry analysis of T-cell surface markers (CD4 and CD8) showed similar subpopulations of T cells in the thymuses of wild type, RNF8 KO and Chfr KO mice. However, compared with the other mice, the percentage of CD4+ CD8+ T cells was increased in the thymuses of DKO mice accompanied by a decrease of single-positive (CD4−CD8+ or CD4+CD8−) thymocytes (Supplementary Figure 2b). Considering the substantial loss of total thymus cellularity in DKO mice, the number of single-positive thymocytes was much less than that in wild type mice. Consistent with the phenotypes observed in the thymus, mature T cells were also reduced in the spleens of DKO mice (Supplementary Figure 2c). These results suggest that RNF8 and Chfr are important for T cell development, which is also consistent with recent studies on the RNF8-deficient mice [30, 31]. Again, the phenotypes of T cell development in DKO mice are very similar to those in ATM-deficient mice [8, 9].

DKO mice and MEFs are hypersensitive to IR

In addition to lymphomagenesis, ATM-deficient mice and cells are hypersensitive to DNA damaging agents, such as IR [8, 9]. To examine whether RNF8 and Chfr function in the ATM pathway, 8-week old wild type, RNF8 KO, Chfr KO and DKO mice were exposed to 8 Gy of IR. We monitored mouse mortality for 4 weeks. During this period, 17% of the wild type and 58% of the Chfr KO mice died, whereas all of the RNF8 KO and DKO mice died (Figure 4a). Compared with RNF8 KO mice, the DKO mice died much earlier. No DKO mice survived beyond 15 days following IR treatment, which is also very similar to the survival seen in ATM −/− mice [8, 9]. Consistent with these results, DKO MEFs were hypersensitive to IR treatment (Figure 4b). Both RNF8 KO MEFs and Chfr KO MEFs showed higher lethality compared with wild type MEFs, but had better viability than DKO MEFs following DNA damage (Figure 4b). Moreover, we also examined metaphase spreads of wild type, RNF8 KO, Chfr KO and DKO MEFs 2 hours after treatment 1 Gy of IR. This assay allows us to quantitatively measure breaks introduced into mitosis, which could lead to chromosome instability. As shown in Figure 4c and Supplementary Figure 3, chromosomal breaks were much more frequently found in DKO MEFs than in wild type MEFs. Compared with wild type MEFs, both RNF8 KO and Chfr KO MEFs had elevated numbers of chromosomal breaks. Taken together, these results indicate that RNF8 and Chfr

synergistically maintain whole body or cell viability and chromosomal stability in response to DNA damage following DSBs.

RNF8 and Chfr synergistically regulate histone ubiquitination and acetylation

Next, we examined the molecular mechanism by which RNF8 and Chfr regulate ATM activation. Since it has been shown that RNF8 regulates histone ubiquitination [14, 16, 32, 33], we examined histone ubiquitination in wild type, RNF8 KO, Chfr KO and DKO MEFs. Compared with that in wild type MEFs, both H2A and H2B ubiquitination were dramatically reduced in DKO MEFs and thymocytes (Figure 5a and b). Histone ubiquitination was also intermediately decreased in RNF8 KO and Chfr KO cells, suggesting that RNF8 and Chfr synergistically regulate global histone ubiquitination. To examine whether RNF8 and Chfr could directly ubiquitinate histones, we performed *in vitro* ubiquitination assays and found that both RNF8 and Chfr function together with UBC13 to ubiquitinate H2A and H2B *in vitro* (Supplementary Figure 4a). Interestingly, although phenotypes observed in Chfr KO mice and MEFs are less dramatically than those in RNF8 KO mice and MEFs, the E3 activity of Chfr is much stronger than that of RNF8 in the *in vitro* ubiquitination assay (Supplementary Figure 4a). However, the mRNA level of Chfr is around one fifth the level of RNF8 in wild type MEFs (Supplementary Figure 4b). Thus, it is likely that different expression level of Chfr and RNF8 in different tissues could provide a layer of regulation for the overlapping function of Chfr and RNF8.

We next examined other histone modifications including several histone methylations and acetylations. Interestingly, compared with that in wild type cells, acetylation of histone H4, but no other histone modifications, was dramatically downregulated in DKO cells (Figure 5a, b and Supplementary Figure 4c). The anti-H4 acetylation antibody we used recognizes acetylation of K5, K8, K12 and K16 at the N-terminal tail of H4. These acetylated lysine residues form a patch with negative charges that may negatively modulate inter-nucleosomal interactions and chromatin decondensation [34–36]. Particularly, H4K16 acetylation is important for chromatin fiber relaxation [37], which regulates ATM activation [38] Similar to histone ubiquitination, global H4K16 acetylation is dramatically reduced in DKO MEFs and thymocytes as well as T-cell lymphomas from DKO mice (Figure 5a, b and c). It has been shown that H4K16 acetylation is up-regulated in response to high dose IR treatment, which is important for ATM activation[38]. Consistently, with relatively low dose IR treatment, we also observed a slight increase of H4K16 acetylation in wild type cells, but not in DKO cells (Supplementary Figure 4d). In addition, nuclei extracted from wild type MEFs were more easily digested by MNase than those in DKO MEFs in the presence or absence of DNA damage (Figure 5d–e and Supplementary Figure 4e–f), indicating that chromatin in wild type MEFs is less compacted than that in DKO MEFs. Collectively, these results are consistent with our recent analyses on spermatogenesis of RNF8 KO mice [33], indicating that RNF8 and Chfr regulate chromatin status through histone ubiquitination-coupled histone acetylation. However, the phenotypes in Chfr single KO cells are relatively weak. To understand the role of Chfr in chromatin remodeling, we transfected DKO cells with wild type Chfr or Ring domain deletion mutant Chfr (ΔRing) that abolishes the E3 ligase activity of Chfr. We found that wild type Chfr but not ΔRing mutant could partially rescue the histone ubiquitination and acetylation as well as ATM activation following DNA damage

(Supplementary Figure 4g–h). These results suggest that the E3 ligase activity of Chfr is important for histone acetylation and ATM activation in response to DNA damage.

Since neither RNF8 nor Chfr have acetyltransferase activity, nor do they associate with any known acetyltransferase (data not shown), loss of H4K16 acetylation could be the sequential effect of loss of histone ubiquitination. H4K16 is mainly acetylated by histone acetyltransferase MOF [38] and Tip60 [39]. Although the overall protein expression of MOF and Tip60 were intact, we found that most of the MOF and Tip60 were dissociated from chromatin in DKO cells (Figure 5f), suggesting that RNF8 and Chfr-dependent histone ubiquitination is required to retain MOF and Tip60 on the chromatin to acetylate H4K16 and facilitate chromatin relaxation.

MRG15 links histone ubiquitination and histone acetylation

In order to elucidate the link between RNF8 and Chfr-dependent histone ubiquitination and H4 acetylation, we studied the mechanism by which RNF8 and Chfr regulate MOF and Tip60. Since chromatin-bound MOF and Tip60 were dramatically reduced in DKO cells (Figure 5f), we wondered whether MOF and Tip60 might recognize RNF8 and Chfr-dependent histone ubiquitination. However, both MOF and Tip60 do not recognize ubiquitinated histones (data not shown). Thus, we screened 11 other known subunits in the MOF and Tip60 complexes [40]. Interestingly, MRG15 (MOF-related gene on chromosome 15), a common subunit in both the MOF and Tip60 complexes [41–43], could interact with ubiquitinated H2B (Ub-H2B), but not non-ubiquitinated H2B (Figure 6a and Supplementary Figure 5a). We generated a series of deletion mutants of MRG15, and found that a region from residue 82 to resudue 262 of MRG15 is required for its interaction with Ub-H2B (Figure 6b). Notably, the region between amino acids 202 and 262 of MRG15 contains triple α-helixes that are very similar to other known ubiquitin-binding motifs [44, 45], and this region alone could bind ubiquitin (Supplementary Figure 5b and c). Moreover, mutation of conserved residues in this ubiquitin-binding motif (I246E and L247E mutant) abolished the interaction between MRG15 and Ub-H2B (Supplementary Figure 5d), suggesting that ubiquitin-binding plays an essential role to mediate the interaction between MRG15 and Ub-H2B. Similar to MOF and Tip60, most of the MRG15 was dissociated from the chromatin in DKO cells (Figure 6c), suggesting that RNF8 and Chfr-dependent histone ubiquitination may retain MOF and Tip60 on the chromatin via MRG15. Depletion of MRG15 by siRNA reduced H4K16 acetylation and chromatin-bound MOF and Tip60, but did not affect H2B ubiquitination (Figure 6d–e and Supplementary Figure 5d–f). Thus, these results suggest that MRG15 recognizes Ub-H2B and stabilizes MOF and Tip60 on the chromatin, facilitating the acetylation of H4K16. Moreover, in the MRG15 depleted cells, ATM activation and phosphorylation of ATM substrates were impaired in response to DSBs (Figure 6f and Supplementary Figure 5g) and only siRNA-resistant wild type MRG15, not the I246E and L247E mutant, could rescue ATM activation in MRG15 depleted cells after DNA damage (Supplementary Figure 5h). Taken together, these results indicate that MRG15 not only mediates histone ubiquitination-coupled histone acetylation but also regulates ATM activation in response to DNA damage.

Suppression of histone deacetylation rescues ATM activation and its related DNA damage response in DKO MEFs

To further examine the role of histone acetylation in RNF8 and Chfr-dependent DNA damage response, cells were treated with trichostatin A (TSA), an inhibitor of class I HDACs, to suppress histone deacetylation. Low dose TSA treatment did not affect H2B ubiquitination, but increased H4K16 acetylation in DKO cells (Figure 7a). More importantly, increased histone acetylation partially restored DNA damage-induced ATM activation in DKO cells (Figure 7a). Correspondingly, TSA treatment facilitated DNA damage repair in DKO cells and partially rescued DKO cell viability following IR treatment (Figure 7b and c).

In addition, 53BP1 is an important downstream mediator of the ATM signaling pathway following DSBs[46]. It has been shown that RNF8 was required for DSB-induced 53BP1 foci formation, although the mechanism of this phenomenon was not clear [14–16]. Interestingly, TSA treatment partially restored 53BP1 foci formation in both RNF8 KO and DKO cells (Figure 7d and Supplementary Figure 6a). TSA alone could not induce DSBs and 53BP1 foci formation in wild type or DKO cells (Supplementary Figure 6b). Taken together, these results suggest that the crosstalk between histone ubiquitination and histone acetylation is important for ATM activation and ATM-dependent DNA damage response.

Discussion

In this study, we demonstrate that RNF8 and Chfr synergistically maintain genomic stability and suppress lymphomagenesis *in vivo*. Both RNF8 and Chfr are important for histone ubiquitination and acetylation, which in turn regulate chromatin structure and ATM-dependent DNA damage response (Figure 8).

The phenotypes of DKO mice are very similar to those of *ATM* −/− mice. For example, DKO and *ATM* −/− mice both develop CD4+ CD8+ T-cell lymphomas. Although the tumor penetrance of DKO mice is lower than that reported in *ATM* −/− mice, spectral karyotype analysis showed similar patterns of chromosome translocations in tumors from DKO mice (Figure 3) and *ATM* −/− mice [11]. Like ATM-deficient mice, DKO mice exhibit impaired T cell development. Since RAG1/2 generates DSBs during T-cell receptor (TCR) V(D)J recombination[47], it is likely that RNF8 and Chfr regulate ATM activation in response to these endogenous DSBs during T cell development. Suppression of ATM activation induces aberrant rearrangements at TCR loci on chromosomes 12 and 14 during TCR V(D)J recombination [8, 9, 11], which is likely to be the mechanism underlying thymic lymphomagenesis in *ATM* −/− and DKO mice. Although other functions of Chfr (non-redundant with RNF8) might play a role during tumorigenesis, the lymphomas identified in DKO mice are diploid or close to diploid with specific chromosome translocation patterns, indicating that abnormal repairs of chromosomal breaks, and not mitotic error-induced aneuploidy, is the major cause of the T-cell lymphomas. It has been shown that Chfr is often silenced in primary tumors or tumor cell lines due to promoter methylation, suggesting that Chfr could be an important tumor suppressor[22, 23]. However, we did not find any evidence of RNF8 silencing when we tested a panel of over 30 human tumor cell lines (data not shown). It is possible that mutations of RNF8 may exist in certain types of tumors or genetic

diseases and Genetic screening of RNF8 mutations in tumor samples will further elucidate the role of RNF8 in human tumor suppression in the future.

Chromatin relaxation facilitates ATM activation in response to DNA damage [25, 48–50]. Here, we found that an important histone modification, H4K16 acetylation, is dramatically downregulated with the loss of both RNF8 and Chfr. Since H4K16 acetylation adds negative charge onto the surface of nucleosomes, it may loosen the chromatin fiber [37]. This chromatin remodeling will allow DDR factors, such as ATM and its partners, to access DNA lesions. In addition, it is very likely that other histone acetylation events cooperate with H4K16 acetylation to relax chromatin fiber at DSBs [50, 51]. Particularly, acetylation of H2A is also reported to facilitate DNA damage response although the detailed mechanism of specific lysine acetylation needs further exploration [39, 52]. Our conclusions are further supported by experiments in which we treated cells with low doses of TSA, an HDAC inhibitor. Low dose TSA treatment could restore H4K16 acetylation in DKO cells by suppressing histone deacetylation, which rescues ATM activation and ATM-dependent DNA damage response. Interestingly, high dose TSA treatment, despite not generating DSBs, could induce ATM auto-phosphorylation even in normal cells by drastically changing chromatin topology [25]. Thus, it is likely that certain chromatin structures and states promote ATM activation. In addition, since chromatin-associated MOF and Tip60, two crucial acyltransferases, are dramatically dissociated from the chromatin in DKO cells, we cannot rule out the effects of other non-histone substrates. It has been shown that acetylation of ATM itself may regulate its activation [51, 53]. However, we did not find any change in ATM acetylation in DKO cells (data not shown).

Previous studies have shown that RNF8 is recruited to DNA damage sites mediated by ATM-dependent MDC1 phosphorylation [14–16]. Although our studies suggest that RNF8 and Chfr control ATM activation in response to DNA damage, these results are not contradicted by previous studies. It is likely that RNF8 and Chfr control the chromatin setting without DNA damage. Indeed, we found that a subset of RNF8 and Chfr is associated with chromatin under normal conditions and there is a substantial increase in chromatin-associated RNF8 and Chfr following DNA damage (Supplementary Figure 7a). Interestingly, the mechanisms for the regulation of chromatin-bound RNF8 and Chfr are slightly different. Under DNA damage conditions, MDC1 is very important for chromatin-associated RNF8 and poly-ADP-ribosylation also modestly affects the chromatin association of RNF8 (Supplementary Figure 7b–c). On the other hand, chromatin-associated Chfr is mainly regulated by poly-ADP-ribosylation and modestly affected in MDC1-deficient cells (Supplementary Figure 7b–c), consistent with the previous finding that Chfr recognizes protein poly-ADP-ribosylation[54]. Moreover, we observed evidence of compensation between Chfr and RNF8, specifically a slight increase in one binding to chromatin if the other is deleted (Supplementary Figure 7d). A detailed molecular mechanism of RNF8 and Chfr on the chromatin needs to be elucidated in the future. Following DNA damage, ATM is activated under the RNF8 and Chfr-dependent chromatin setting and phosphorylates H2AX and MDC1, which forms a positive feedback loop to recruit more RNF8 to DNA damage sites and relax local chromatin fibers at the DNA lesion. This feedback loop can amplify the DNA damage-induced signals for cell cycle checkpoint activation and facilitate DNA damage repair.

Down-regulation of H4K16 acetylation is a hallmark of human cancers, including cancer cells derived from leukemia/lymphoma [55]. Besides being considered as a biomarker of human cancers, loss of H4K16 acetylation could trigger or promote tumorigenesis by abrogation of ATM-dependent DNA damage response. Clearly, the effects of TSA on H4K16 actetlyation and ATM-dependent DNA damage response indicate that HDAC inhibitors may be very useful for future tumor prevention and therapeutics.

In this study, we have demonstrated a new trans-histone modification. The status of histone ubiquitination correlates with histone H4K16 acetylation in wild type and DKO MEFs. Moreover, the level of Ub-H2A and Ub-H2B also correlates to the level of chromatin-association of MOF and Tip60. These results are similar to what we previously reported in the analysis of RNF8-deficient testes [33]. It has been shown that the N-terminal tail of H4, including H4K16 site, from one nucleosome interacts with a H2A/H2B heterodimer on an adjacent nucleosome [34]. Thus, it is possible that the bulky ubiquitin group may simply change the internucleosomal space to expose the lysine residues of H4 for acetylation. We found that MRG15, a common subunit of MOF and Tip60 complexes [41–43], recognizes H2B ubiquitination and is likely to stabilize acetyltransferases on the chromatin to catalyze histone acetylation. Moreover, It has been shown that MRG15 regulates H4 acetylation and plays an important role in the DNA damage response [42]. We also noticed that a appreciable portion of Tip60 still associates with the chromatin in DKO cells. Since the chromo domain of Tip60 interacts with other histone methylations [56], other partners of Tip60 complexes may also recognize Ub-H2B (or Ub-H2A) or other ubiquitinated proteins in response to DNA damage and facilitate H4K16 acetylation.

In summary, we have shown that RNF8 and Chfr, two chromatin remodelers, synergistically maintain chromatin stability and suppress lymphomagenesis by regulating ATM-dependent DNA damage response.

Mmethods

Generation of DKO mice

Male RNF8 +/− mice were bred with female Chfr −/− mice to generate double heterozygous offspring (RNF8 +/− Chfr +/−). These mice were internally crossed to generate wild type (RNF8 +/+ Chfr +/+), RNF8 KO (RNF8 −/− Chfr +/+), Chfr KO (RNF8 +/+ Chfr −/−) and DKO (RNF8 −/− Chfr −/−) mice. Genomic DNA extracted from mouse tail was used for genotyping by PCR as previously described[33, 57] Mice were observed daily and moribund mice were sacrificed for tumor analysis.

Cell Culture, IR and TSA treatment

Wild type, RNF8 KO, Chfr KO and DKO MEFs were generated from E13.5 mouse embryos using standard procedure and cultured in DMEM media with 10% (v/v) FBS. For IR treatment, cells were irradiated with a JL Spepherd ^{137}Cs radiation source at indicated doses. Following IR treatment, cells were maintained in the culture conditions for indicated time points specified in the figure legends. For whole body irradiation, 8-week old wild type, RNF8 KO, Chfr KO and DKO mice were irradiated with 8 Gy. The mice were monitored

for morbidity and mortality for 4 weeks. For TSA treatment, cells were incubated with 0.2 μM TSA for 12 hours before exposure to IR.

In vitro kinase assay

Cells were treated with 10 Gy of IR and allowed to recover for 1 hour at 37°C. Irradiated cells were lysed with NTN 300 buffer (without EDTA). ATM was purified using anti-ATM antibody and protein G beads at 4 °C. After three washes with kinase buffer (10 mM HEPES Ph 7.5, 50 mM glycerophosphate, 50 mM NaCl, 10 mM MgCl, 10 mM MnCl, and 1 mM DTT), the beads were incubated with purified GST-p53 (a.a. 1–250) in the kinase buffer with or without ATP at 37°C for 30 minutes. Proteins were eluted with SDS loading buffer, separated by SDS-PAGE and analyzed by Western blot using the indicated antibodies.

Metaphase spread and spectral karyotype (SKY) analysis

To prepare metaphase spread, thymic tumor cells were cultured in RPMI 1640 medium with 10% (v/v) FBS and incubated in 0.1 mg/ml KaryoMAX colcemid solution (GIBCO) for 3 hours. Cells were collected, washed with PBS, resuspended in 75 mM KCl and incubated at room temperature for 15 minutes. Then cells were fixed with Carnoy's solution (75% (v/v) methanol and 25% (v/v) acetic acid) and dropped onto glass slides. SKY analyses were performed using a mouse SKY probe kit (Applied Spectral Imaging, Vista, CA) according to the manufacturer's protocol, followed by counter-staining with DAPI. Metaphase images were captured using the Olympus BX-61 microscope equipped with a CCD camera (Applied Spectral Imaging, Vista, CA) and analyzed by SKYview software (Applied Spectral Imaging, Vista, CA).

Analysis of IR-induced chromosomal breaks

Freshly prepared MEFs (passage 0) were treated with 1 Gy of IR and allowed to recover for 2 hours. Metaphase spreads were prepared and stained with 5% (w/v) Giemsa solution. Metaphase spreads were observed under a light microscope with a 100 × oil objective lens, and chromosome breaks were counted.

G2/M checkpoint assay

MEFs were irradiated with or without 2 Gy of IR. After one hour of recovery, cells were fixed with 70% (v/v) ethanol and stained with rabbit anti-phospho-histone H3 (pSer10) antibody, followed by incubation with FITC-conjugated goat anti-rabbit secondary antibody. The stained cells were treated with RNase A and then incubated with propidium iodide. Samples were analyzed by flow cytometry.

G1/S checkpoint assay

MEFs were treated with or without 6 Gy of IR. Six hours after treatment, cells were pulsed with 40 mM BrdU for 30 minutes, then harvested and washed with PBS. Cells were fixed in 70% (v/v) ethanol for 30 minutes. After fixation, cells were washed with PBS and then treated with 2 M HCl for 30 minutes at room temperature. The low pH was neutralized by spinning and resuspending cell pellets in 0.1 M sodium tetraborate (pH 8.5). Cells were stained with anti-BrdU antibody (BD Biosciences) in the dark for 30 minutes and then

incubated with corresponding secondary antibodies. The stained cells were treated with RNase A and incubated with propidium iodide. Samples were analyzed by flow cytometry.

Micrococcal nuclease sensitivity assay

Micrococcal nuclease (MNase) sensitivity assay was carried out as described [58]. Briefly, MEFs were washed with cold PBS and lysed with nuclei extraction (NE) buffer (10 mM Tris-HCL, pH 8.0, 0.1 mM EDTA, 2 mM MgCl2, 2 mM CaCl2, 1 mM DTT, 0.2 % (v/v) NP-40) on ice. The resultant nuclei were washed with NE buffer twice, suspended in NE buffer and digested at 25°C for 5 minutes with 1 U/ml of MNase. The reaction was stopped by adding stop buffer (50 mM Tris-HCL, pH 8.0, 25 mM EDTA, 1 % (w/v) SDS). DNA was purified by incubation with 200 μg ml^{-1} of proteinase K for 1 hour at 55 °C, followed by phenol-chloroform extraction and ethanol precipitation. The DNA was resuspended in TE buffer and separated by agarose gel electrophoresis, stained by ethidium bromide (EtBr). Each line of the EtBr gels was scanned and profiles representing band intensity were obtained using the NIH IMAGE J software. Average size of oligonucleosomes was calculated as described [58].

Supplementary Material

Refer to Web version on PubMed Central for supplementary material.

Acknowledgments

We are grateful to Drs. Eric Fearon, Kathleen Cho, Benjamin Margolis, Dou Yali and Liu Yang at university of Michigan for sharing of experimental equipment and reagents. We also thank Dr. Jennifer Keller for proofreading of the manuscript. This work was supported by the American Cancer Society (RSG-08-125-01-CCG to X.Y.) and the National Institute of Health (CA132755 and CA130899 to X.Y.). X.Y. is a recipient of the Era of Hope Scholar Award from the Department of Defense.

References

1. Rouse J, Jackson SP. Interfaces between the detection, signaling, and repair of DNA damage. Science (New York, NY). 2002; 297:547–551.
2. Harper JW, Elledge SJ. The DNA damage response: ten years after. Molecular cell. 2007; 28:739–745. [PubMed: 18082599]
3. Jackson SP, Bartek J. The DNA-damage response in human biology and disease. Nature. 2009; 461:1071–1078. [PubMed: 19847258]
4. Khanna KK, Lavin MF, Jackson SP, Mulhern TD. ATM, a central controller of cellular responses to DNA damage. Cell death and differentiation. 2001; 8:1052–1065. [PubMed: 11687884]
5. Rotman G, Shiloh Y. ATM: a mediator of multiple responses to genotoxic stress. Oncogene. 1999; 18:6135–6144. [PubMed: 10557105]
6. Harrison JC, Haber JE. Surviving the breakup: the DNA damage checkpoint. Annual review of genetics. 2006; 40:209–235.
7. Lavin MF. Ataxia-telangiectasia: from a rare disorder to a paradigm for cell signalling and cancer. Nature reviews. 2008; 9:759–769.
8. Barlow C, et al. Atm-deficient mice: a paradigm of ataxia telangiectasia. Cell. 1996; 86:159–171. [PubMed: 8689683]
9. Xu Y, et al. Targeted disruption of ATM leads to growth retardation, chromosomal fragmentation during meiosis, immune defects, and thymic lymphoma. Genes & development. 1996; 10:2411–2422. [PubMed: 8843194]

10. Taylor AM, Metcalfe JA, Thick J, Mak YF. Leukemia and lymphoma in ataxia telangiectasia. Blood. 1996; 87:423–438. [PubMed: 8555463]
11. Liyanage M, et al. Abnormal rearrangement within the alpha/delta T-cell receptor locus in lymphomas from Atm-deficient mice. Blood. 2000; 96:1940–1946. [PubMed: 10961898]
12. Panier S, Durocher D. Regulatory ubiquitylation in response to DNA double-strand breaks. DNA repair. 2009; 8:436–443. [PubMed: 19230794]
13. Bennett EJ, Harper JW. DNA damage: ubiquitin marks the spot. Nature structural & molecular biology. 2008; 15:20–22.
14. Huen MS, et al. RNF8 transduces the DNA-damage signal via histone ubiquitylation and checkpoint protein assembly. Cell. 2007; 131:901–914. [PubMed: 18001825]
15. Kolas NK, et al. Orchestration of the DNA-damage response by the RNF8 ubiquitin ligase. Science (New York, NY). 2007; 318:1637–1640.
16. Mailand N, et al. RNF8 ubiquitylates histones at DNA double-strand breaks and promotes assembly of repair proteins. Cell. 2007; 131:887–900. [PubMed: 18001824]
17. Wang B, Elledge SJ. Ubc13/Rnf8 ubiquitin ligases control foci formation of the Rap80/Abraxas/Brca1/Brcc36 complex in response to DNA damage. Proceedings of the National Academy of Sciences of the United States of America. 2007; 104:20759–20763. [PubMed: 18077395]
18. Ito K, et al. N-Terminally extended human ubiquitin-conjugating enzymes (E2s) mediate the ubiquitination of RING-finger proteins, ARA54 and RNF8. European journal of biochemistry / FEBS. 2001; 268:2725–2732. [PubMed: 11322894]
19. Zhao GY, et al. A critical role for the ubiquitin-conjugating enzyme Ubc13 in initiating homologous recombination. Molecular cell. 2007; 25:663–675. [PubMed: 17349954]
20. Brooks L 3rd, Heimsath EG Jr, Loring GL, Brenner C. FHA-RING ubiquitin ligases in cell division cycle control. Cell Mol Life Sci. 2008; 65:3458–3466. [PubMed: 18597043]
21. Bothos J, Summers MK, Venere M, Scolnick DM, Halazonetis TD. The Chfr mitotic checkpoint protein functions with Ubc13-Mms2 to form Lys63-linked polyubiquitin chains. Oncogene. 2003; 22:7101–7107. [PubMed: 14562038]
22. Mizuno K, et al. Aberrant hypermethylation of the CHFR prophase checkpoint gene in human lung cancers. Oncogene. 2002; 21:2328–2333. [PubMed: 11948416]
23. Toyota M, et al. Epigenetic inactivation of CHFR in human tumors. Proceedings of the National Academy of Sciences of the United States of America. 2003; 100:7818–7823. [PubMed: 12810945]
24. Huen MS, et al. Noncanonical E2 variant-independent function of UBC13 in promoting checkpoint protein assembly. Molecular and cellular biology. 2008; 28:6104–6112. [PubMed: 18678647]
25. Bakkenist CJ, Kastan MB. DNA damage activates ATM through intermolecular autophosphorylation and dimer dissociation. Nature. 2003; 421:499–506. [PubMed: 12556884]
26. Bertholon J, et al. Chfr inactivation is not associated to chromosomal instability in colon cancers. Oncogene. 2003; 22:8956–8960. [PubMed: 14654793]
27. Lefrancois D, Kokalj N, Viegas-Pequignot E, Montagnier L, Dutrillaux B. High recurrence of rearrangements involving chromosome 14 in an ataxia telangiectasia lymphoblastoid cell line and in its mutagen-treated derivatives. Human genetics. 1991; 86:475–480. [PubMed: 1849869]
28. Davey MP, et al. Juxtaposition of the T-cell receptor alpha-chain locus (14q11) and a region (14q32) of potential importance in leukemogenesis by a 14;14 translocation in a patient with T-cell chronic lymphocytic leukemia and ataxia-telangiectasia. Proceedings of the National Academy of Sciences of the United States of America. 1988; 85:9287–9291. [PubMed: 3194425]
29. Baer R, et al. The breakpoint of an inversion of chromosome 14 in a T-cell leukemia: sequences downstream of the immunoglobulin heavy chain locus are implicated in tumorigenesis. Proceedings of the National Academy of Sciences of the United States of America. 1987; 84:9069–9073. [PubMed: 3122210]
30. Li L, et al. Rnf8 deficiency impairs class switch recombination, spermatogenesis, and genomic integrity and predisposes for cancer. The Journal of experimental medicine. 207:983–997. [PubMed: 20385750]
31. Santos MA, et al. Class switching and meiotic defects in mice lacking the E3 ubiquitin ligase RNF8. The Journal of experimental medicine. 207:973–981. [PubMed: 20385748]

32. Wu J, et al. Histone ubiquitination associates with BRCA1-dependent DNA damage response. Molecular and cellular biology. 2009; 29:849–860. [PubMed: 19015238]
33. Lu LY, et al. RNF8-dependent histone modifications regulate nucleosome removal during spermatogenesis. Developmental cell. 18:371–384. [PubMed: 20153262]
34. Luger K, Mader AW, Richmond RK, Sargent DF, Richmond TJ. Crystal structure of the nucleosome core particle at 2.8 A resolution. Nature. 1997; 389:251–260. [PubMed: 9305837]
35. Dorigo B, Schalch T, Bystricky K, Richmond TJ. Chromatin fiber folding: requirement for the histone H4 N-terminal tail. Journal of molecular biology. 2003; 327:85–96. [PubMed: 12614610]
36. Gordon F, Luger K, Hansen JC. The core histone N-terminal tail domains function independently and additively during salt-dependent oligomerization of nucleosomal arrays. The Journal of biological chemistry. 2005; 280:33701–33706. [PubMed: 16033758]
37. Shogren-Knaak M, et al. Histone H4-K16 acetylation controls chromatin structure and protein interactions. Science (New York, NY). 2006; 311:844–847.
38. Rea S, Xouri G, Akhtar A. Males absent on the first (MOF): from flies to humans. Oncogene. 2007; 26:5385–5394. [PubMed: 17694080]
39. Kusch T, et al. Acetylation by Tip60 is required for selective histone variant exchange at DNA lesions. Science (New York, NY). 2004; 306:2084–2087.
40. Lee KK, Workman JL. Histone acetyltransferase complexes: one size doesn't fit all. Nature reviews. 2007; 8:284–295.
41. Cai Y, et al. Identification of new subunits of the multiprotein mammalian TRRAP/TIP60-containing histone acetyltransferase complex. The Journal of biological chemistry. 2003; 278:42733–42736. [PubMed: 12963728]
42. Garcia SN, Kirtane BM, Podlutsky AJ, Pereira-Smith OM, Tominaga K. Mrg15 null and heterozygous mouse embryonic fibroblasts exhibit DNA-repair defects post exposure to gamma ionizing radiation. FEBS letters. 2007; 581:5275–5281. [PubMed: 17961556]
43. Pardo PS, Leung JK, Lucchesi JC, Pereira-Smith OM. MRG15, a novel chromodomain protein, is present in two distinct multiprotein complexes involved in transcriptional activation. The Journal of biological chemistry. 2002; 277:50860–50866. [PubMed: 12397079]
44. Prag G, et al. Mechanism of ubiquitin recognition by the CUE domain of Vps9p. Cell. 2003; 113:609–620. [PubMed: 12787502]
45. Mueller TD, Feigon J. Solution structures of UBA domains reveal a conserved hydrophobic surface for protein-protein interactions. Journal of molecular biology. 2002; 319:1243–1255. [PubMed: 12079361]
46. Zgheib O, et al. ATM signaling and 53BP1. Radiother Oncol. 2005; 76:119–122. [PubMed: 16024119]
47. Bassing CH, Swat W, Alt FW. The mechanism and regulation of chromosomal V(D)J recombination. Cell. 2002; 109 (Suppl):S45–55. [PubMed: 11983152]
48. Shiotani B, Zou L. Single-stranded DNA orchestrates an ATM-to-ATR switch at DNA breaks. Molecular cell. 2009; 33:547–558. [PubMed: 19285939]
49. You Z, Bailis JM, Johnson SA, Dilworth SM, Hunter T. Rapid activation of ATM on DNA flanking double-strand breaks. Nature cell biology. 2007; 9:1311–1318. [PubMed: 17952060]
50. Kim YC, et al. Activation of ATM depends on chromatin interactions occurring before induction of DNA damage. Nature cell biology. 2009; 11:92–96. [PubMed: 19079244]
51. Murr R, et al. Histone acetylation by Trrap-Tip60 modulates loading of repair proteins and repair of DNA double-strand breaks. Nature cell biology. 2006; 8:91–99. [PubMed: 16341205]
52. Ikura T, et al. DNA damage-dependent acetylation and ubiquitination of H2AX enhances chromatin dynamics. Molecular and cellular biology. 2007; 27:7028–7040. [PubMed: 17709392]
53. Sun Y, Jiang X, Chen S, Fernandes N, Price BD. A role for the Tip60 histone acetyltransferase in the acetylation and activation of ATM. Proceedings of the National Academy of Sciences of the United States of America. 2005; 102:13182–13187. [PubMed: 16141325]
54. Ahel I, et al. Poly(ADP-ribose)-binding zinc finger motifs in DNA repair/checkpoint proteins. Nature. 2008; 451:81–85. [PubMed: 18172500]

55. Fraga MF, et al. Loss of acetylation at Lys16 and trimethylation at Lys20 of histone H4 is a common hallmark of human cancer. Nature genetics. 2005; 37:391–400. [PubMed: 15765097]

56. Sun Y, et al. Histone H3 methylation links DNA damage detection to activation of the tumour suppressor Tip60. Nature cell biology. 2009; 11:1376–1382. [PubMed: 19783983]

57. Yu X, et al. Chfr is required for tumor suppression and Aurora A regulation. Nature genetics. 2005; 37:401–406. [PubMed: 15793587]

58. Ziv Y, et al. Chromatin relaxation in response to DNA double-strand breaks is modulated by a novel ATM- and KAP-1 dependent pathway. Nature cell biology. 2006; 8:870–876. [PubMed: 16862143]

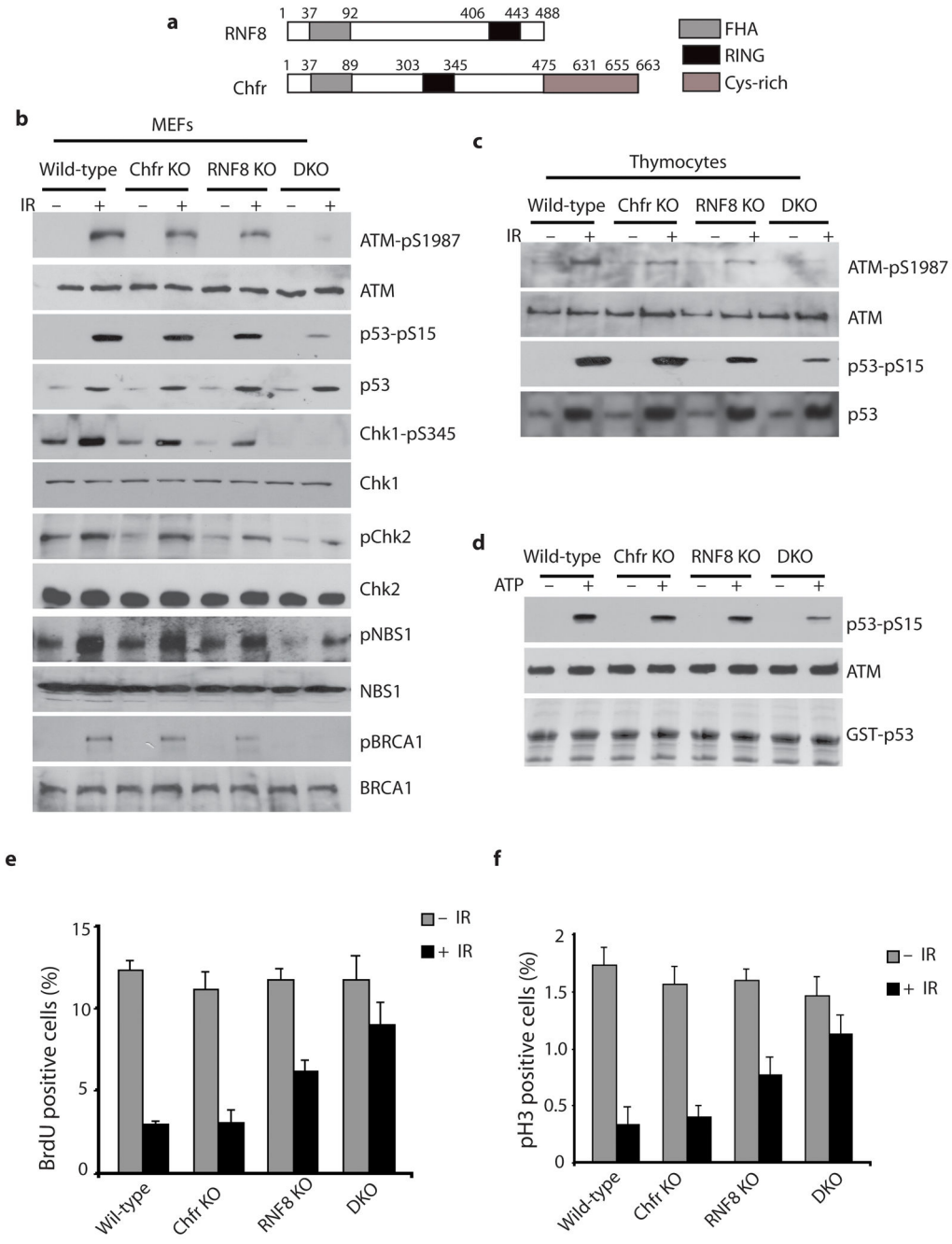

Figure 1. DNA damage-induced ATM signaling pathway is impaired in DKO cells

(a) Domain architecture of mouse RNF8 and Chfr. (b and c) RNF8 and Chfr synergistically regulate ATM auto-phosphorylation and the ATM-dependent signaling pathway following DNA damage. MEFs (b) and Thymocytes (c) were treated with or without IR, lysed and subjected to Western blot using the indicated antibodies. (d) Chfr and RNF8 synergistically regulate ATM kinase activity. *In vitro* kinase assay was separated by SDS-PAGE and subjected to Western blot. Coomassie Brilliant Blue (CBB) staining is shown below for loading control. (e) RNF8 and Chfr double deficiency abrogates G1/S checkpoint activation. BrdU assay was performed and mean values were calculated from three independent

experiments. Error bar represent s.e.m. (f) DNA damage-induced G2/M checkpoint is abrogated in DKO cells. G2/M checkpoint assay was performed and mean values were calculated from three independent experiments. Error bar represent s.e.m.

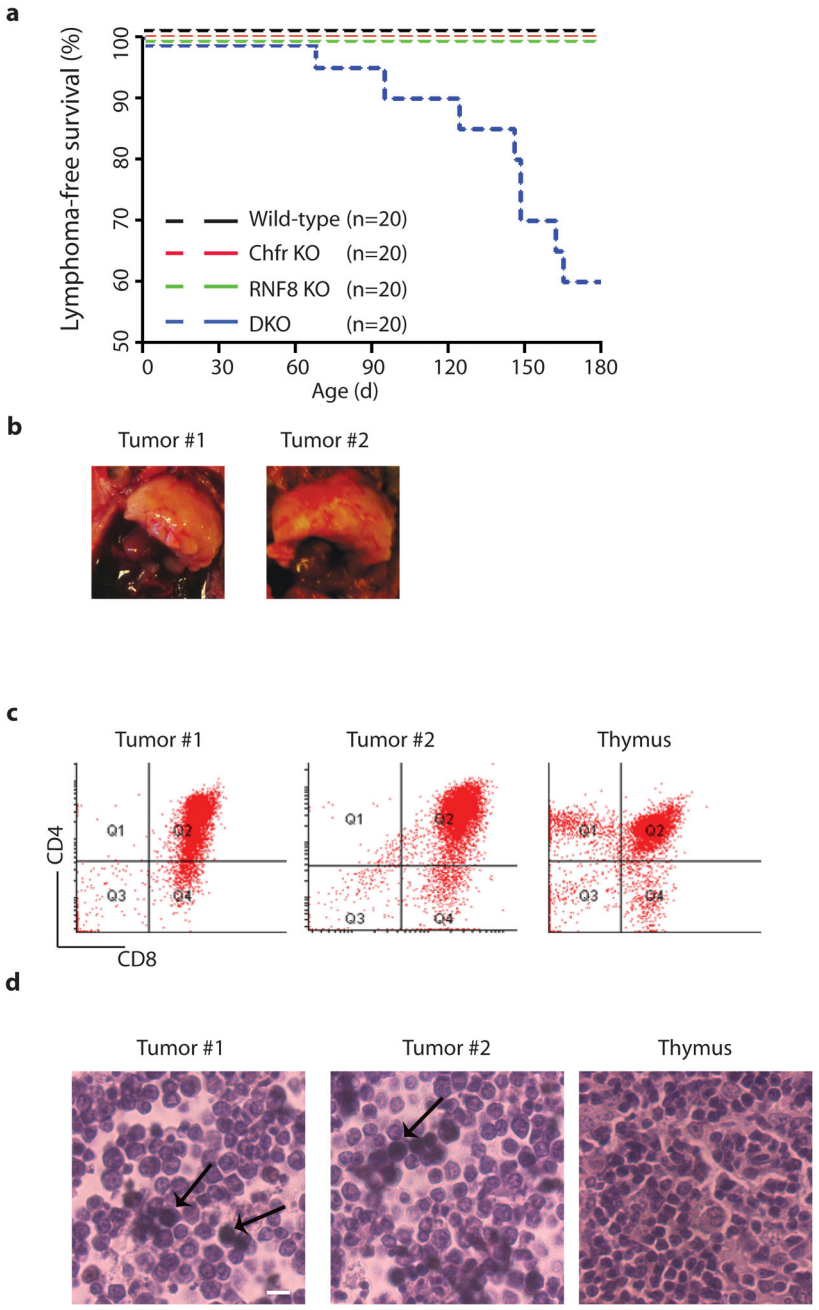

Figure 2. RNF8 and Chfr double-deficient mice develop T-cell lymphoma

(a) Lymphoma-free survival rate of mice over 6 months. (b) Massive thymic lymphomas harvested from DKO mice. (c) Thymocytes from wild type mice and tumors were analyzed by flow cytometry. (d) Hematoxylin-and-eosin-stained sections from DKO thymic lymphomas and wild type thymus. Arrows indicate mitotic figures.

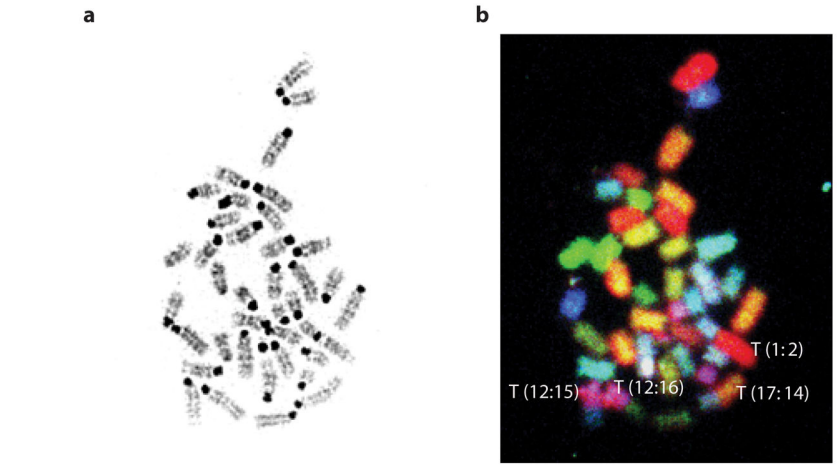

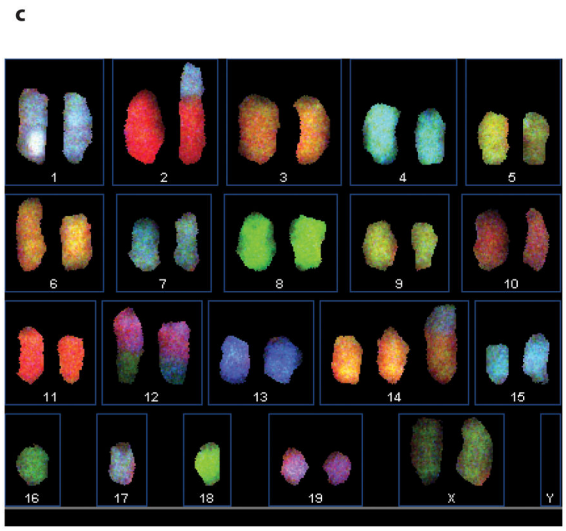

d

Karyotypes of T-cell lymphomas

Tumor	No of chromosome	Clonal translocations
#1	38	T (2; 1)
		T (12; 15)
		T (12; 16)
		T (17; 14)
#2	39	T (10; 1)
		T (12; 16)
		T (12; 1)
		T (6; 7)
#3	40	T (13; 12)
		T (14; 12)
		T (12; 1)
		T (3; 15)
#4	40	T (14; 3)
		T (13; 12)
		T (19; X)
#5	39	T (2; 1)
		T (12; 15)
		T (12; 16)
		T (17; 6)

Figure 3. Thymic lymphomas from DKO mice harbor clonal translocations

(a) A representative metaphase spread of lymphoma #1 is shown by DAPI staining. (b) The SKY image of the metaphase spread is shown, with translocations indicated. (c) Representative karyotype from lymphoma #1. (d) Summary of chromosome translocations in DKO lymphomas.

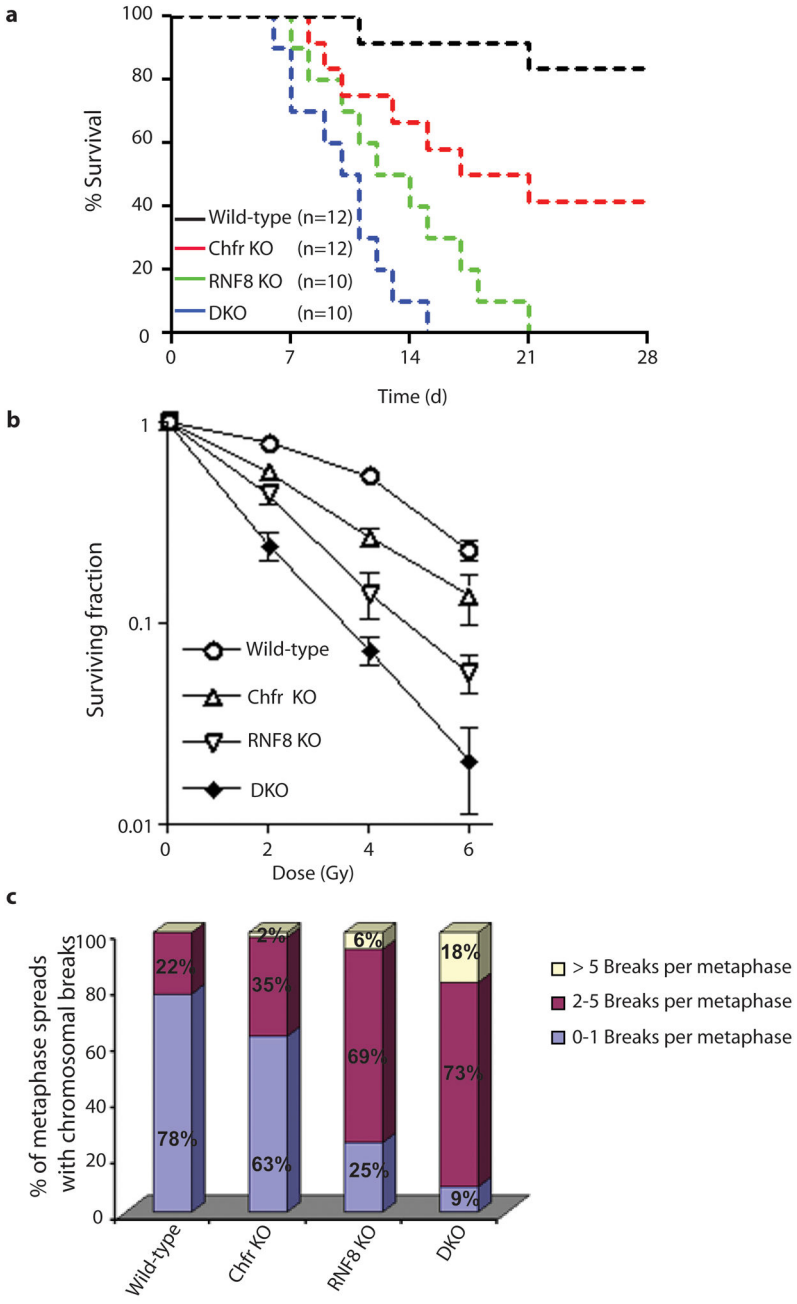

Figure 4. DKO mice and MEFs are hypersensitive to IR

(a) Survival of mice treated with 8 Gy of IR at 8-weeks (b) DKO MEFs are hypersensitive to IR. MEFs were treated with IR at the indicated doses and counted after 10 days. The ratio between IR-treated and mock-irradiated cells of the same genotype is shown. Results represent the mean value from three independent experiments. Error bar represent s.e.m. (c) Chromosome breaks in mitotic DKO MEFs are elevated following IR treatment. MEFs were treated with 1 Gy of IR. Chromosome breaks were counted in each metaphase spread. 100 metaphase spreads were examined for each genotype.

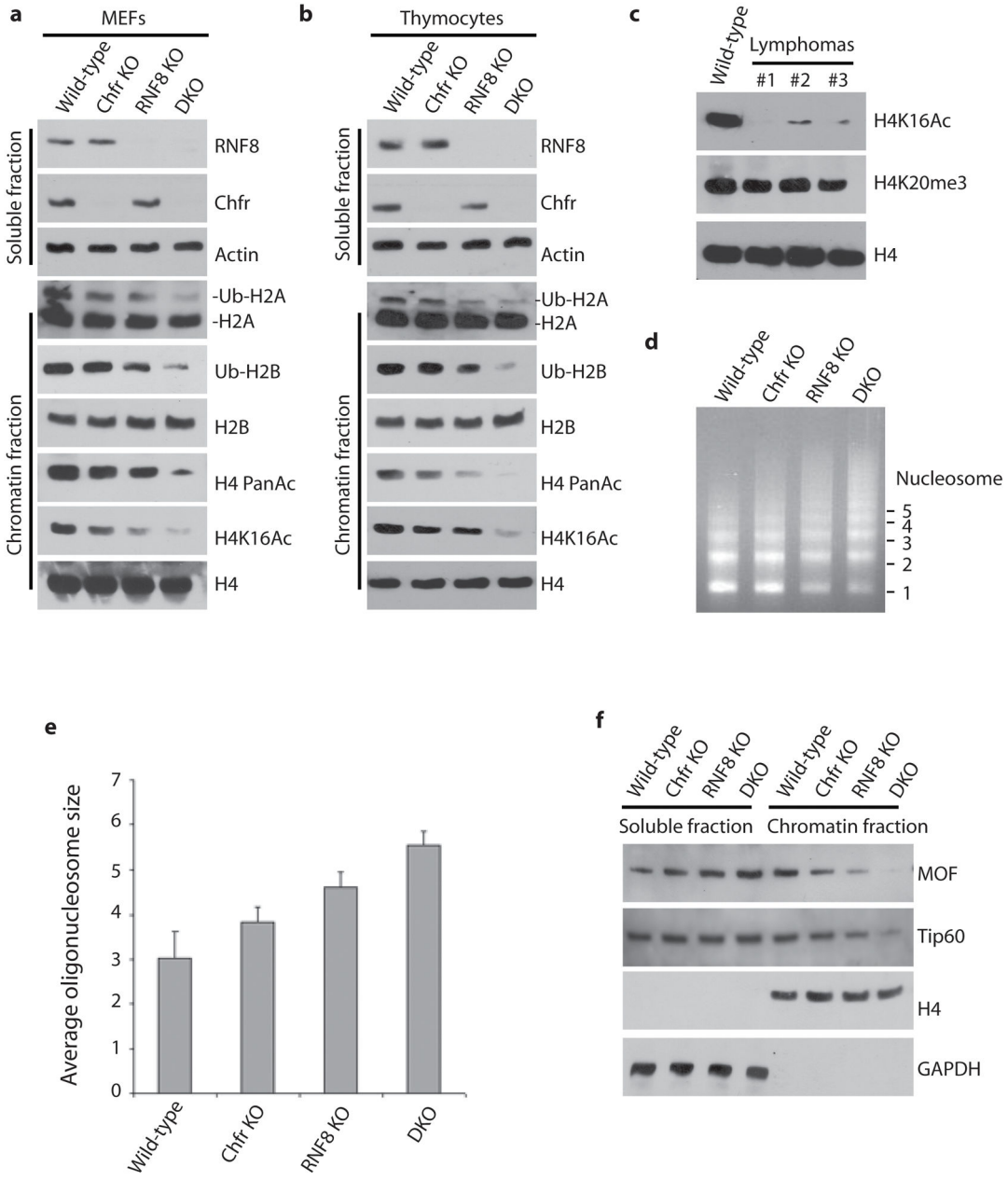

Figure 5. RNF8 and Chfr synergistically regulate histone ubiquitination and acetylation

(a and b) Ub-H2A, Ub-H2B and H4K16 acetylation are decreased in DKO MEFs and thymocytes from DKO mice. Soluble and chromatin fractions were extracted from MEFs (a) or thymocytes (b) and analyzed by Western blot using the indicated antibodies. (c) H4K16 acetylation is down-regulated in DKO lymphomas. Chromatin fractions from three different DKO lymphomas and wild type thymus were analyzed by Western blot. (d and e) Chromatin relaxation is impaired in DKO cells. MNase sensitivity assay was performed. Average length of oligonucleosome was calculated from three independent experiments. Error bar represent s.e.m. (f) Chromatin-associated MOF and Tip60 are reduced in DKO MEFs. The

soluble and chromatin fractions were prepared from MEFs and analyzed by Western blot using the indicated antibodies

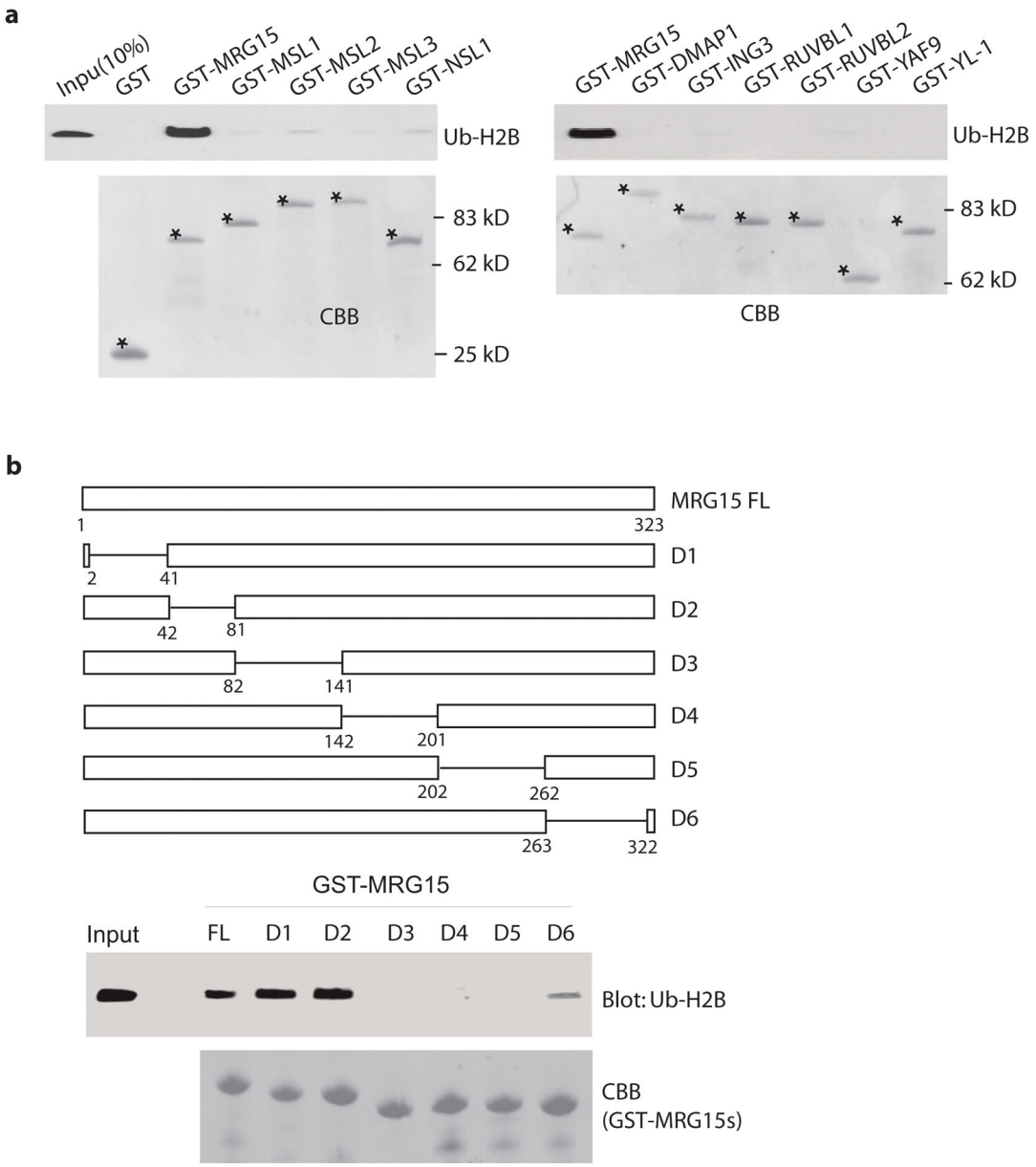

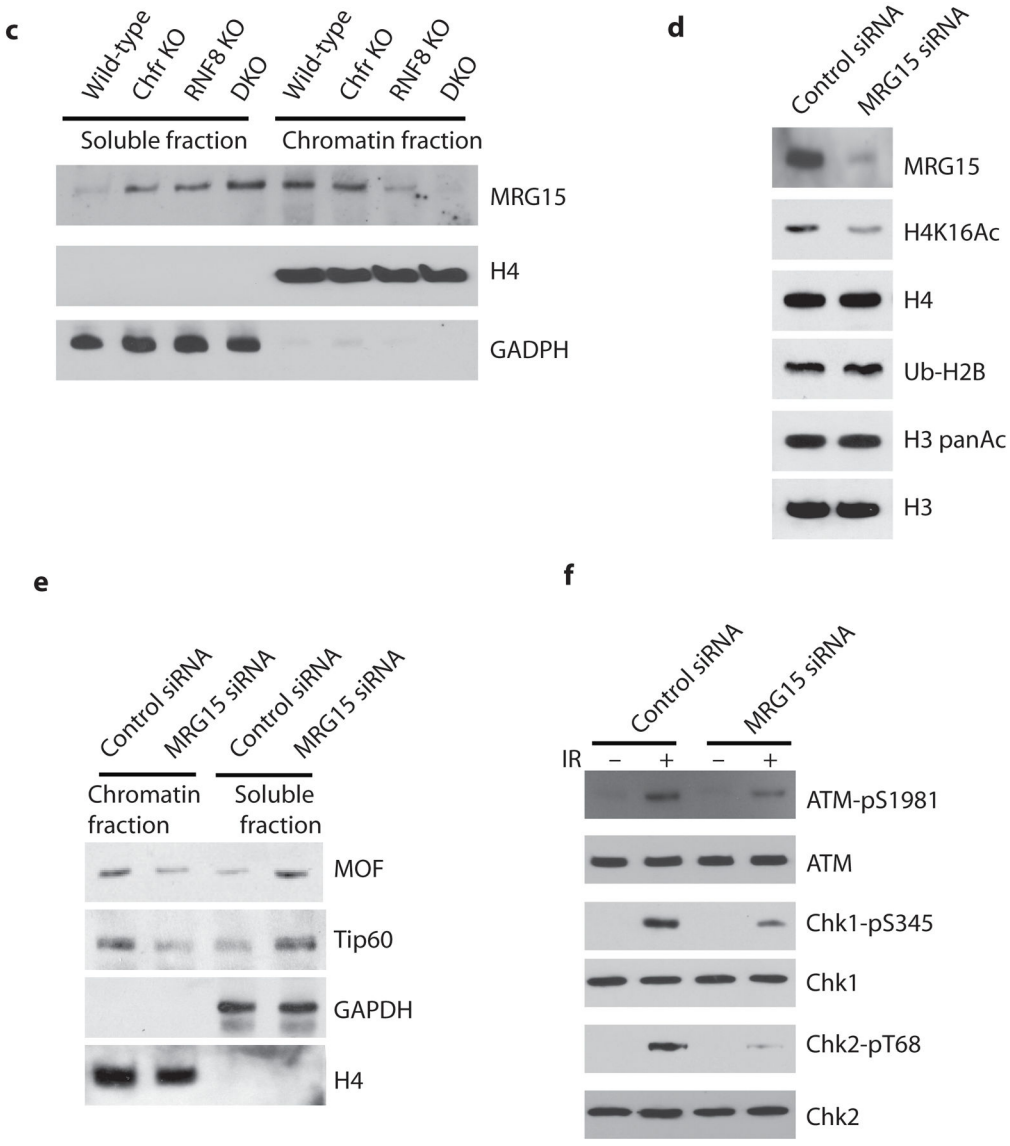

Figure 6. MRG15 links histone H2B ubiquitination and H4K16 acetylation

(a) MRG15 associates with Ub-H2B. The GST or GST fusion proteins associated proteins were analyzed by immunoblotting with anti-Ub-H2B antibody. CBB staining is shown below for loading control. (b) A region from a.a. 82 to 262 of MRG15 recognizes Ub-H2B. The MRG15 or its mutants associated proteins were analyzed by immunoblotting with anti-Ub-H2B antibody. CBB staining is shown below for loading control. (c) Chromatin-associated MRG15 is dramatically reduced in DKO MEFs. The soluble and chromatin fractions were prepared from MEFs and subjected to Western blot. (d) Depletion of MRG15 affects H4K16 acetylation. Chromatin-bound proteins from control siRNA or MRG15 siRNA-treated U2OS cells were analyzed by Western blot. (e) Chromatin-associated MOF and Tip60 were decreased in MRG15-depleted cells. Soluble and chromatin fractions were extracted from control siRNA or MRG15 siRNA-treated U2OS cells and analyzed by Western blot. (F) The ATM-dependent DNA damage response pathway is impaired in

MRG15-depleted cells. Control siRNA or MRG15 siRNA-treated U2OS cells were irradiated with or without 10 Gy of IR. One hour after IR treatment, cell lysates were examined by Western blot.

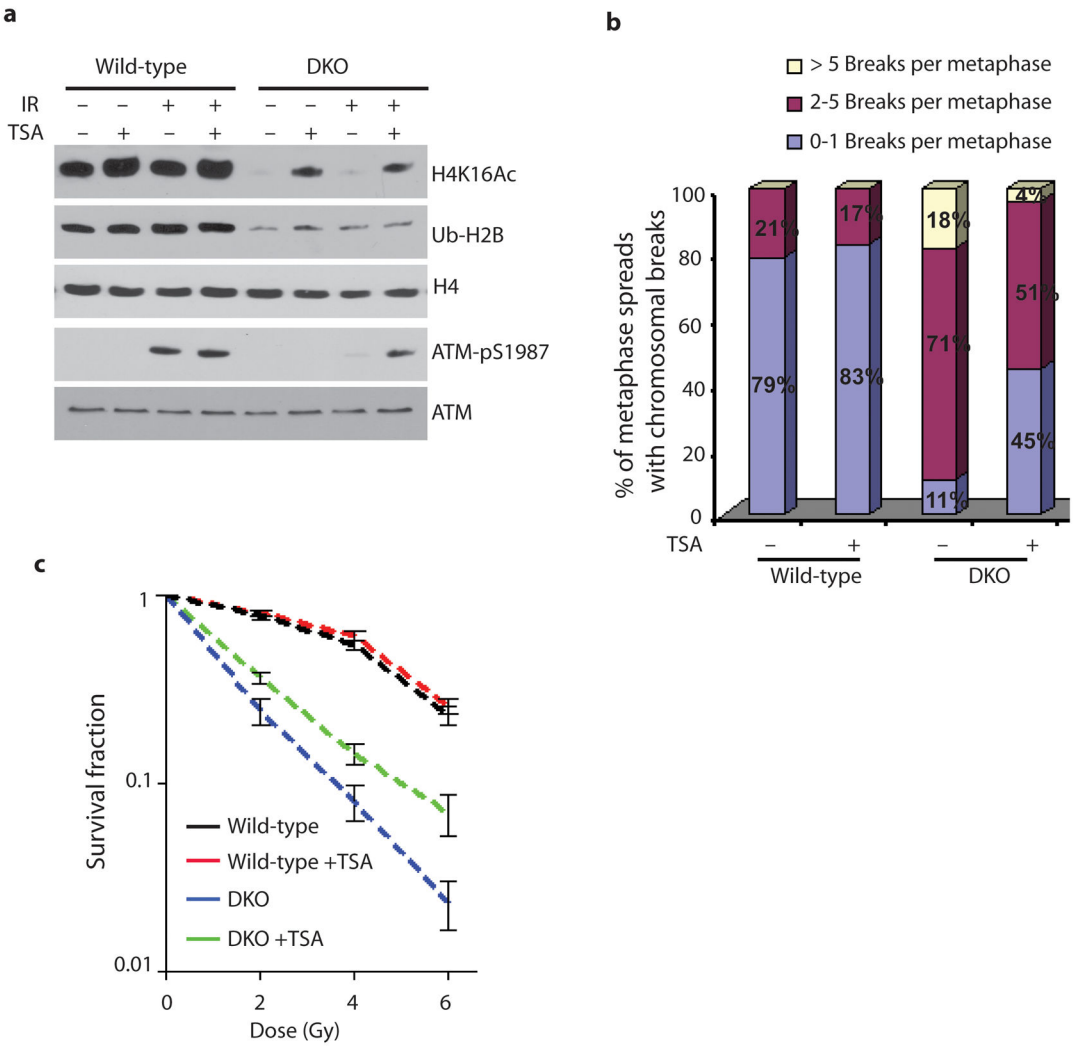

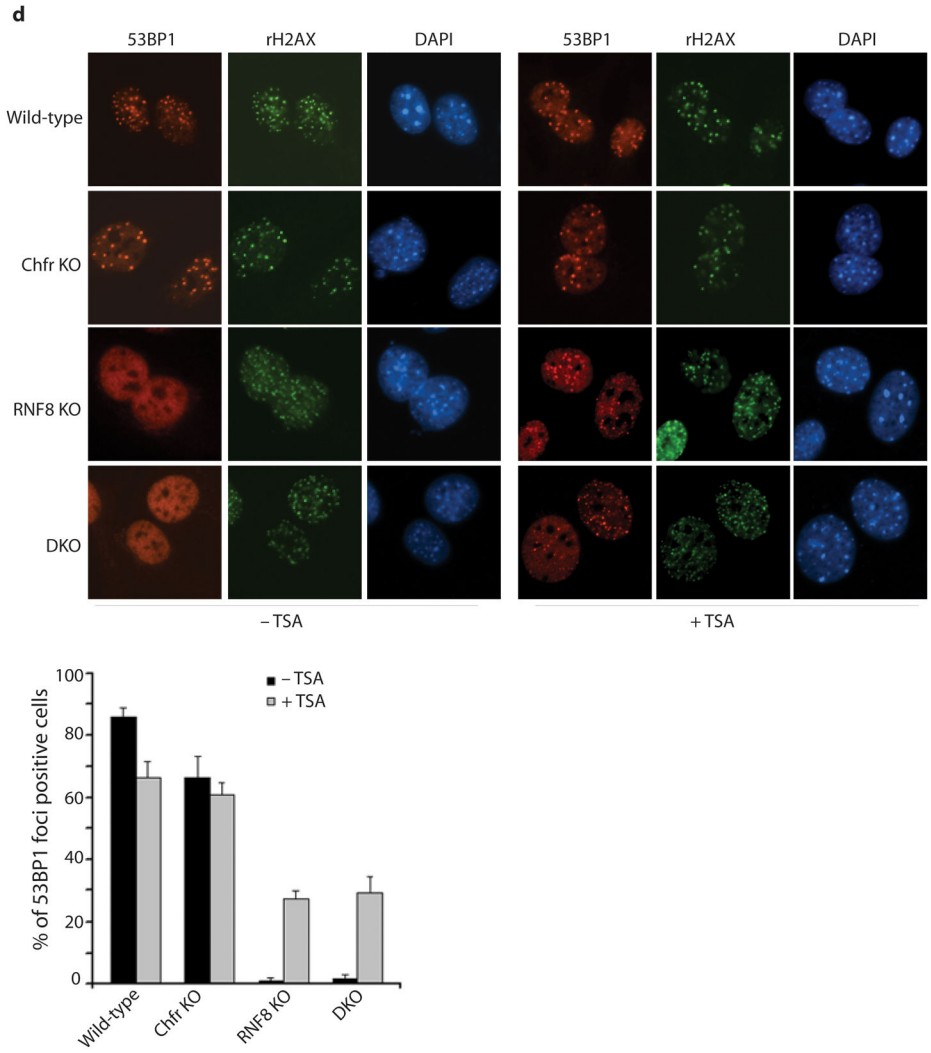

Figure 7. Suppression of histone acetylation rescues ATM-dependent DNA damage response in DKO MEFs

(a) TSA treatment restores the ATM-dependent signaling pathway in DKO cells. Cells were treated with TSA and IR as described in methods. Cell lysates were subjected to Western blot. (b) TSA treatment reduced IR-induced chromosome breaks in DKO cells. Cells were treated with TSA and IR as described in methods. Chromosome breaks were counted in metaphase spreads, with 100 metaphases evaluated for each genotype. (c) TSA treatment increases DKO cell survival following DNA damage. Cells were treated with TSA and IR followed by colony formation assay. Results were calculated from three independent experiments. Error bar represent s.e.m. (d) TSA treatment partially restores IR-induced 53BP1 foci formation in RNF8 KO and DKO cells. Cells were treated with TSA and IR as described in methods. Cells were fixed and immunostained with indicated antibodies. Histogram indicates percentage of 53BP1 foci-positive cells. Error bar represent s.e.m. from three independent experiments.

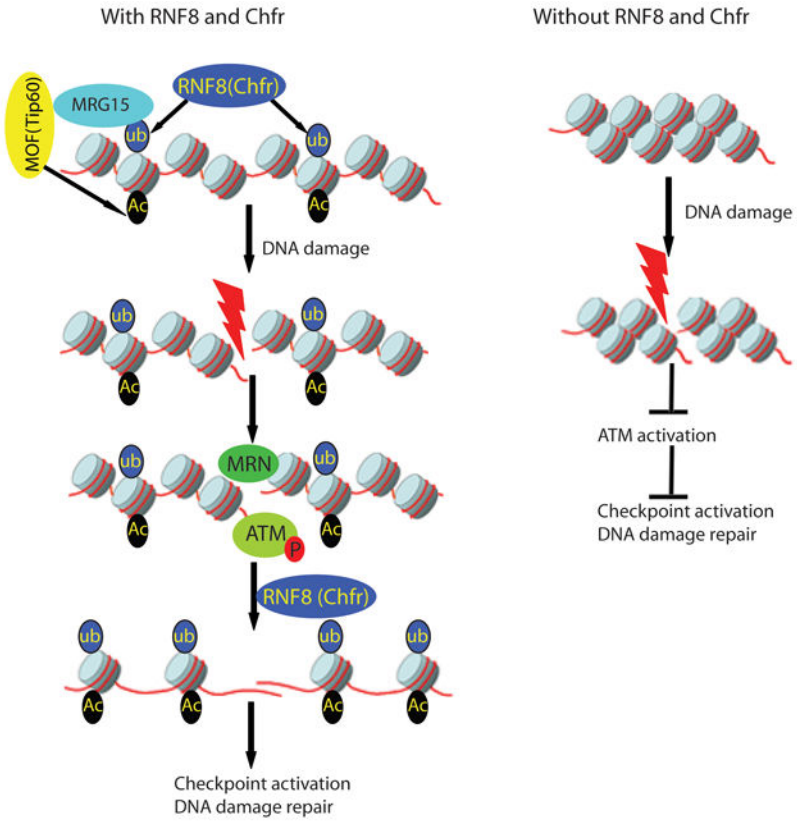

Figure 8.

A model of histone modifications, chromatin relaxation and ATM activation following DNA damage. RNF8 and Chfr are important for histone ubiquitination and acetylation that in turn induce chromatin relaxation, which facilitates ATM activation and ATM-dependent DNA damage response following DNA damage.